Engineering Analysis with Boundary Elements 132 (2021) 263–270

Contents lists available at ScienceDirect

Engineering Analysis with Boundary Elements

journal homepage: www.elsevier.com/locate/enganabound

An efficient approach for solving nonlinear multidimensional Schrödinger equations

Neslişah İmamoğlu Karabaş [a], Sıla Övgü Korkut [b], Gamze Tanoğlu [a], Imran Aziz [c,*], Siraj-ul-Islam [d]

[a] Izmir Institute of Technology, Gülbahçe Campus, Urla, İzmir, 35430, Turkey
[b] Department of Engineering Sciences, Izmir Kâtip Çelebi University, Balatçık Campus, Çiğli, İzmir, 35620, Turkey
[c] Department of Mathematics, University of Peshawar, Pakistan
[d] Department of Basic Sciences, Faculty of Architecture Allied Sciences and Humanities, University of Engineering and Technology, Peshawar, Pakistan

ARTICLE INFO

Keywords:
Cubic nonlinear Schrödinger equation
Meshless method
Fréchet derivative

ABSTRACT

An efficient numerical method is proposed for the solution of the nonlinear cubic Schrödinger equation. The proposed method is based on the Fréchet derivative and the meshless method with radial basis functions. An important characteristic of the method is that it can be extended from one-dimensional problems to multi-dimensional ones easily. By using the Fréchet derivative and Newton–Raphson technique, the nonlinear equation is converted into a set of linear algebraic equations which are solved iteratively. Numerical examples reveal that the proposed method is efficient and reliable with respect to the accuracy and stability.

1. Introduction

Schrödinger equation plays an essential role to predict the energy of the quantum mechanical system. Thus, it is an important equation both in physics and in engineering contexts. Among different types of Schrödinger equations, cubic nonlinear Schrödinger equation has got central importance due to its many applications. Several phenomena in physics and engineering can be modelled using cubic nonlinear Schrödinger equation.

An important type of nonlinear Schrödinger equation is the equation with the cubic nonlinear term $(|\psi|^2\psi)$ which is called the cubic nonlinear Schrödinger equation and is given as follows:

$$i\frac{\partial\psi(t,\mathbf{x})}{\partial t} = \left(-\alpha\Delta + \beta|\psi(t,\mathbf{x})|^2 + \omega(\mathbf{x})\right)\psi(t,\mathbf{x}),\ (t,\mathbf{x}) \in (0,T]\times\Omega \qquad (1)$$

subjects to either Dirichlet or Neumann boundary conditions and with an initial condition

$$\psi(0,\mathbf{x}) = \psi_0(\mathbf{x}),\ x \in \Omega$$

where $\psi(t,\mathbf{x})$ is the complex valued function, t is the time variable, α is a positive constant, β is a constant, $\Omega \subset \mathbf{R}^d$ is a bounded domain. The external potential function $\omega(x)$ is a real-valued function.

Solving nonlinear Schrödinger equation analytically is difficult and sometimes impossible. Therefore, several researchers have worked on numerical solution of Schrödinger equations: Subaşı has applied finite difference schemes for the numerical solution of two-dimensional Schrödinger equation [1]. Bratsos has used a linearized Crank–Nicolson scheme for numerical solution of nonlinear cubic Schrödinger equation [2]. Wu has used Dufort–Frankel-type methods for solving linear and nonlinear Schrödinger equations [3]. Dehghan and Taleei have applied a compact split-step finite difference method for solving the nonlinear Schrödinger equations [4]. Dehghan has presented finite difference procedures for solving two-dimensional Schrödinger equation [5]. Taleei and Dehghan have applied a time splitting pseudo-spectral domain decomposition method [6] for solving the nonlinear Schrödinger equations. Quintic B-spline Galerkin finite element method has been applied to nonlinear Schrödinger equation for Neumann type boundary condition [7], exponential cubic B-spline finite element method has been considered in [8].

Recently, there has been an improvement for the space discretization technique which is called meshless method. Since the classical mesh based methods such as finite difference, finite element and finite volume methods are not appropriate for all types of domains, the meshless method has become more attractive in the numerical investigations. There are several types of meshless methods which have been applied for numerical solution of linear and nonlinear partial differential equations. Due to its easy application, meshless method with radial basis is the most important one among various types. The studies on meshless collocation method with radial basis functions can be found in the Refs. [9–17].

* Corresponding author.
E-mail address: imran_aziz@uop.edu.pk (I. Aziz).

https://doi.org/10.1016/j.enganabound.2021.07.009
Received 25 December 2020; Received in revised form 6 June 2021; Accepted 22 July 2021
Available online 12 August 2021

In the present work, a numerical solution of cubic nonlinear Schrödinger equation in both one- and two-dimensional cases is proposed. In order to tackle the nonlinearity, Fréchet derivative technique [18] is applied as a tool. The essential idea behind the process is Newton–Raphson iterative process combining with the Fréchet derivative. In so doing, nonlinear equation is converted into a linear one. After that, to obtain the numerical solution, the meshless method with radial basis function is applied for spatial discretization and Crank–Nicolson method is applied for time discretization.

The outline of this paper is as follows. Section 2.1 is dedicated to the introduction of the proposed linearized method. In Section 2.2, the meshless method with radial basis function will be described. Numerical tests and simulations for the proposed linearized method will be considered in Section 3. In Section 4, some conclusions of the proposed work will be drawn.

2. Construction of the method

2.1. Linearization technique

The essential idea of the proposed method is Newton–Raphson iterative process via Fréchet derivatives. To introduce this method briefly, we first consider the general nonlinear differential equation as follows:

$$L(U) = 0, \tag{2}$$

where L is a differential operator. The solution of Eq. (2) can be described in the following form:

$$U^{n+1} = U^n + \theta^n. \tag{3}$$

Here n corresponds to the iteration number and θ^n corresponds to the refinement variable for correcting function U^n. Primarily, for solving refinement variable, we deal with the following differential equation

$$\theta^n L'(U^n) + L(U^n) = 0. \tag{4}$$

By means of the definition of Fréchet derivative, the term $\theta^n L'(U^n)$ is defined as

$$\theta^n L'(U^n) = \frac{\partial}{\partial \varepsilon} L(U^n + \varepsilon \theta^n)\Big|_{\varepsilon=0}. \tag{5}$$

The above formulation can easily be extended to systems of partial differential equations. As the cubic nonlinear Schrödinger equation can be expressed as a system of two partial differential equations by separating the real and imaginary parts, therefore, we consider the case of two partial differential equations only in this paper. Thus, we have the system containing two nonlinear partial differential equations. That is,

$$\begin{aligned} L_1(U,V) &= 0, \\ L_2(U,V) &= 0. \end{aligned} \tag{6}$$

Due to the Newton–Raphson method, the solution of Eq. (6) can be expressed as

$$\begin{aligned} U^{n+1} &= U^n + {\theta_1}^n, \\ V^{n+1} &= V^n + {\theta_2}^n, \end{aligned} \tag{7}$$

where, as mentioned before, ${\theta_1}^n$ and ${\theta_2}^n$ which are the refinements corresponding to the iteration number n are obtained by dealing with the following differential equations:

$$\begin{aligned} {\theta_1}^n {L_1}'(U^n,V^n) + {\theta_2}^n {L_1}'(U^n,V^n) + L_1(U^n,V^n) &= 0, \\ {\theta_1}^n {L_2}'(U^n,V^n) + {\theta_2}^n {L_2}'(U^n,V^n) + L_2(U^n,V^n) &= 0. \end{aligned} \tag{8}$$

After applying Fréchet derivatives to get ${\theta_i}^n {L_j}'(U^n,V^n)$, $i,j = 1,2$,

$$\begin{aligned} {\theta_1}^n {L_i}'(U^n,V^n) &= \frac{\partial}{\partial \varepsilon} L_i\left(U^n + \varepsilon {\theta_1}^n, V^n\right)\Big|_{\varepsilon=0}, \\ {\theta_2}^n {L_i}'(U^n,V^n) &= \frac{\partial}{\partial \varepsilon} L_i\left(U^n, V^n + \varepsilon {\theta_2}^n\right)\Big|_{\varepsilon=0}, \end{aligned} \tag{9}$$

the linearized form can be easily obtained. Assuming $\psi(t,\mathbf{x}) = U(t,\mathbf{x}) + iV(t,\mathbf{x})$, the cubic nonlinear Schrödinger equation can be expressed as a system of two partial differential equations as follows:

$$\begin{aligned} L_1(U,V) &= U_t + \alpha \Delta V - \beta\left(U^2 + V^2\right)V - \omega V = 0, \\ L_2(U,V) &= V_t - \alpha \Delta U + \beta\left(U^2 + V^2\right)U + \omega U = 0. \end{aligned} \tag{10}$$

Applying the linearization technique to the system given in Eq. (10) one can obtain

$$\theta^n_{1_t} + \alpha \Delta \theta^n_2 - 2\beta U^n V^n \theta^n_1 - \beta\left((U^n)^2 + 3(V^n)^2\right)\theta^n_2 - \omega \theta^n_2 + L_1(U^n,V^n) = 0, \tag{11}$$

$$\theta^n_{2_t} - \alpha \Delta \theta^n_1 + \beta\left(3(U^n)^2 + (V^n)^2\right)\theta^n_1 + 2\beta U^n V^n \theta^n_2 + \omega \theta^n_1 + L_2(U^n,V^n) = 0. \tag{12}$$

Here Eqs. (11) and (12) are linear with respect to the θ_1 and θ_2. Matrix notations of Eqs. (11) and (12) can be written as follows:

$$\Theta^n_t + \alpha A \Theta^n + B\Theta^n + \beta C(U^n,V^n)\Theta^n = -\Psi^n_t - \alpha A \Psi^n - B\Psi^n - \beta D(|\Psi^n|)\Psi^n \tag{13}$$

where $\Theta = [\theta_1, \theta_2]^T$ and $\Psi = [U,V]^T$. Moreover,

$$A = \begin{bmatrix} \mathbf{0} & \sum_{i=1}^{d} \frac{\partial^2}{\partial x_i^2} \\ -\sum_{i=1}^{d} \frac{\partial^2}{\partial x_i^2} & \mathbf{0} \end{bmatrix}, \quad B = \begin{bmatrix} \mathbf{0} & -\boldsymbol{\omega} \\ \boldsymbol{\omega} & \mathbf{0} \end{bmatrix} \tag{14}$$

$$\begin{aligned} C(U,V) &= \begin{bmatrix} -2UV & -(U^2 + 3V^2) \\ (3U^2 + V^2) & 2UV \end{bmatrix}, \\ D(|\psi|) &= \begin{bmatrix} \mathbf{0} & -(U^2 + V^2) \\ (U^2 + V^2) & \mathbf{0} \end{bmatrix}. \end{aligned} \tag{15}$$

Notice that the operator $\sum_{i=1}^{d} \frac{\partial^2}{\partial x_i^2}$ will be approximated by the meshless method with radial basis functions. Moreover, $\mathbf{0}$ denotes the zero matrix and $\boldsymbol{\omega} = \omega \boldsymbol{I}$ where $\boldsymbol{I}$ stands for the identity matrix. Applying the Crank–Nicolson method to Eq. (13) one can obtain

$$\begin{aligned} \frac{\Theta^n_{m+1} - \Theta^n_m}{\Delta t} + \alpha A \frac{\Theta^n_{m+1} + \Theta^n_m}{2} + B\frac{\Theta^n_{m+1} + \Theta^n_m}{2} \\ + \beta C\left(U^n_{m+1}, V^n_{m+1}\right)\frac{\Theta^n_{m+1} + \Theta^n_m}{2} \\ = -\frac{\Psi^n_{m+1} - \Psi^n_m}{\Delta t} - \alpha A \frac{\Psi^n_{m+1} + \Psi^n_m}{2} - B\frac{\Psi^n_{m+1} + \Psi^n_m}{2} \\ - \beta D\left(\left|\frac{\Psi^n_{m+1} + \Psi^n_m}{2}\right|\right)\frac{\Psi^n_{m+1} + \Psi^n_m}{2}, \end{aligned}$$

where $t_{m+1} = t_0 + m\Delta t$, $\Theta^n_{m+1} = \Theta^n(t_{m+1})$, $\Psi^n_{m+1} = \Psi^n(t_{m+1})$ and Δt is the time step.

2.2. Meshless method with radial basis functions

There are several types of radial basis functions, however, multiquadric radial basis function (MQ RBF) is the most commonly used among all radial basis functions and we will use MQ RBF in this paper. In this approach, the formulation of the problem starts with the representation of the unknown function $\psi(\mathbf{x})$ with MQ RBF on the entire domain. The derivatives are then calculated by differentiation of the MQ RBF function. The RBF approximation for $\psi(\mathbf{x})$ is given in the following form:

$$\psi(\mathbf{x}) \simeq \sum_{k=1}^{N} \phi(r,c)\lambda_k, \quad \mathbf{x} \in \mathbf{R}^d, \tag{16}$$

where $\lambda_k, k = 1,2,\ldots,N$ are the RBF's coefficients and

$$r = \|\mathbf{x} - \mathbf{x_k}\|_2 = \sqrt{(x_1 - x_{k_1})^2 + \cdots + (x_d - x_{k_d})^2}.$$

The MQ RBF is defined as

$$\phi(r,c) = \sqrt{r^2 + c^2}, \tag{17}$$

where c is the shape parameter. It is important to note that the shape parameter has a crucial role on the convergence and accuracy of the meshless method.

The variables U and V can be approximated as follows:

$$U(\mathbf{x}) \simeq \sum_{k=1}^{N} \phi(r,c_1)\lambda_k, \tag{18}$$

and

$$V(\mathbf{x}) \simeq \sum_{k=1}^{N} \phi(r,c_2)\gamma_k, \tag{19}$$

where ϕ is MQ radial basis function. The unknown parameters λ_k and γ_k, $k = 1,2,\dots,N$ can be found using the collocation points in the following form:

$$U(\mathbf{x}_i) = \sum_{k=1}^{N} \phi(r_{ik},c_1)\lambda_k, \tag{20}$$

$$V(\mathbf{x}_i) = \sum_{k=1}^{N} \phi(r_{ik},c_2)\gamma_k,\ i = 1,\dots,N. \tag{21}$$

where $r = \sqrt{(x_1 - x_{k_1})^2 + \cdots + (x_d - x_{k_d})^2}$. Eqs. (20) and (21) can be written in matrix form as:

$$\mathbf{U} = \mathbf{A}_\mathbf{U}\lambda, \tag{22}$$

and

$$\mathbf{V} = \mathbf{A}_\mathbf{V}\gamma, \tag{23}$$

where

$$\mathbf{A}_\mathbf{U} = \begin{bmatrix} \phi(r_{11},c_1) & \phi(r_{12},c_1) & \dots & \phi(r_{1N},c_1) \\ \phi(r_{21},c_1) & \phi(r_{22},c_1) & \dots & \phi(r_{2N},c_1) \\ \cdot & \cdot & \cdot & \cdot \\ \cdot & \cdot & \cdot & \cdot \\ \phi(r_{N1},c_1) & \phi(r_{N2},c_1) & \dots & \phi(r_{NN},c_1) \end{bmatrix},$$

$$\mathbf{A}_\mathbf{V} = \begin{bmatrix} \phi(r_{11},c_2) & \phi(r_{12},c_2) & \dots & \phi(r_{1N},c_2) \\ \phi(r_{21},c_2) & \phi(r_{22},c_2) & \dots & \phi(r_{2N},c_2) \\ \cdot & \cdot & \cdot & \cdot \\ \cdot & \cdot & \cdot & \cdot \\ \phi(r_{N1},c_2) & \phi(r_{N2},c_2) & \dots & \phi(r_{NN},c_2) \end{bmatrix},$$

$r_{ik} = \sqrt{(x_{i_1} - x_{k_1})^2 + \cdots + (x_{i_d} - x_{k_d})^2}$, $\lambda = [\lambda_1,\lambda_2,\dots,\lambda_N]^T$ and $\gamma = [\gamma_1,\gamma_2,\dots,\gamma_N]^T$. Therefore,

$$\lambda = \mathbf{A}_\mathbf{U}{}^{-1}\mathbf{U}, \tag{24}$$

and

$$\gamma = \mathbf{A}_\mathbf{V}{}^{-1}\mathbf{V}. \tag{25}$$

RBF approximations for the derivatives of variables U and V can be represented by

$$\frac{\partial^2 U(x_i)}{\partial x_j^2} \simeq \sum_{k=1}^{N} \frac{\partial^2}{\partial x_j^2}\phi(r_{ik},c_1)\lambda_k, \tag{26}$$

and

$$\frac{\partial^2 V(x_i)}{\partial x_j^2} \simeq \sum_{k=1}^{N} \frac{\partial^2}{\partial x_j^2}\phi(r_{ik},c_2)\gamma_k. \tag{27}$$

The differentiation matrices can be defined as

$$D_U = H_1\mathbf{A}_\mathbf{U}{}^{-1}, \tag{28}$$

and

$$D_V = H_2\mathbf{A}_\mathbf{V}{}^{-1}, \tag{29}$$

where the entries of H_1 and H_2 are

$$h_{1_{ik}} = \frac{\partial^2}{\partial x_j^2}\phi(r_{ik},c_1),$$

and

$$h_{2_{ik}} = \frac{\partial^2}{\partial x_j^2}\phi(r_{ik},c_2),$$

$k,i = 1,2,\dots,N$.

3. Numerical examples and simulations

In this section, we will apply the proposed method to benchmark problems from the literature. It is crucial to note that any numerical method developed for solving solitary wave equations must preserve some physical characteristics of solitary waves such as structural behaviour, mass, and energy conservation. To test the validity of any numerical method on solitary wave conservation of both mass and energy is also required to confirm. The mass and energy conservations are mathematically defined as

$$M(t) := \int_\Omega |\psi|^2 dx := M(0), \tag{30}$$

$$E(t) := \frac{1}{2}\int_\Omega \left(\alpha|\nabla\psi|^2 + \omega(\mathbf{x})|\psi|^2 + \frac{\beta}{2}|\psi|^4\right)dx := E(0). \tag{31}$$

In discrete space, mass and energy conservations can be expressed as follows:

$$EMC = \Delta x \sum_{k=1}^{N_x} |M_k^n - M_k^0|, \tag{32}$$

$$EEC = \Delta x \sum_{k=1}^{N_x} (E_k^n - E_k^0). \tag{33}$$

Here, EMC and EEC denote the errors of mass conservation and of energy conservation, respectively. Moreover, E^0 and M^0 denote the initial energy and initial mass, respectively. Then, from Eqs. (30) and (31), we have

$$E_i^n = \frac{\alpha}{2}((a_i^n)^2 + (b_i^n)^2) + \frac{\omega(x_i)}{2}((V_i^n)^2 + (U_i^n)^2) + \frac{\beta}{4}((V_i^n)^2 + (U_i^n)^2)^2, \tag{34}$$

$$M_i^n = (V_i^n)^2 + (U_i^n)^2, \tag{35}$$

where $a = \nabla U$, $b = \nabla V$ for $\Psi = U + iV$ and E_i^n is the energy at $t = n\Delta t$ and $x = x_i$. It is important to state that throughout the section we have essentially focused on the above-mentioned characteristics.

3.1. One-dimensional cubic nonlinear Schrödinger equation

As our first example, we consider the one-dimensional cubic nonlinear Schrödinger equation:

$$i\psi_t + \psi_{xx} + |\psi|^2\psi = 0, \tag{36}$$

$$\psi(x_L,t) = \psi(x_R,t) = 0,$$

the initial condition is taken as

$$\psi(x,0) = \sqrt{2}\,\mathrm{sech}(x+10)e^{ix/4}, \tag{37}$$

where $\psi(x,t)$ denotes the probability amplitude for the particle to be found at position x at time t, $x_L = -20$ and $x_R = 5$. In order to solve the equation we put it into system form by considering $\psi = U + iV$ in Eq. (36).

Here, the exact solution is given in [19] as

$$\psi(x,t) = \sqrt{2}\,\mathrm{sech}\left(x - \frac{t}{2} + 10\right)e^{i\left(\frac{x}{4} + \frac{15}{16}t\right)}. \tag{38}$$

The numerical results are shown in Fig. 1. One important property of the solitary waves is that they can travel without changing their whole structure and energy, which is evident from this figure. On the other

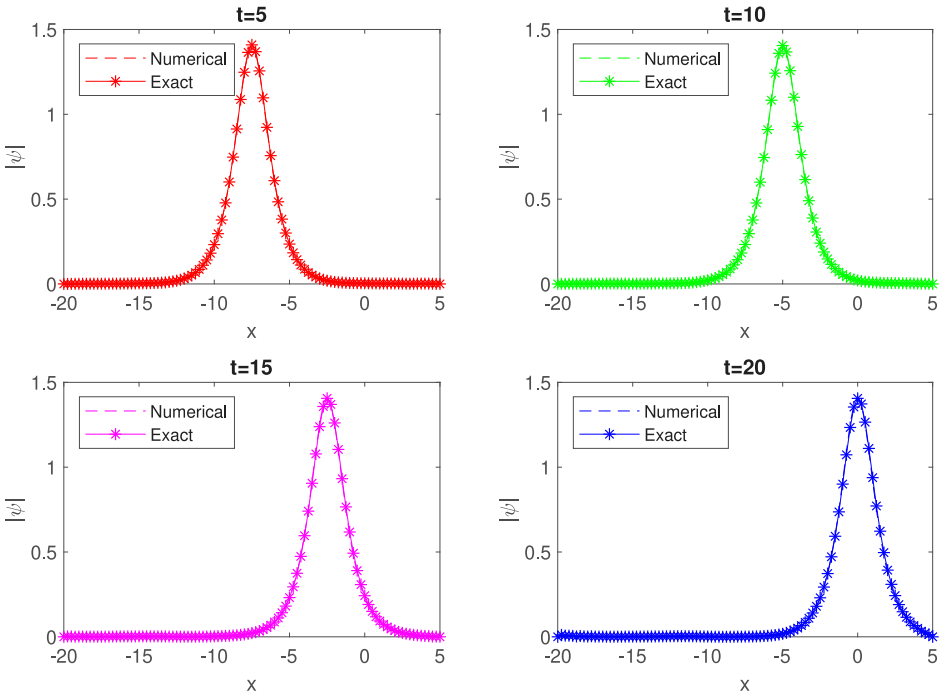

Fig. 1. Exact and numerical solutions of Eq. (36) for $N = 100$ and $c_1 = c_2 = 0.5$ at a certain time for Problem 3.1.

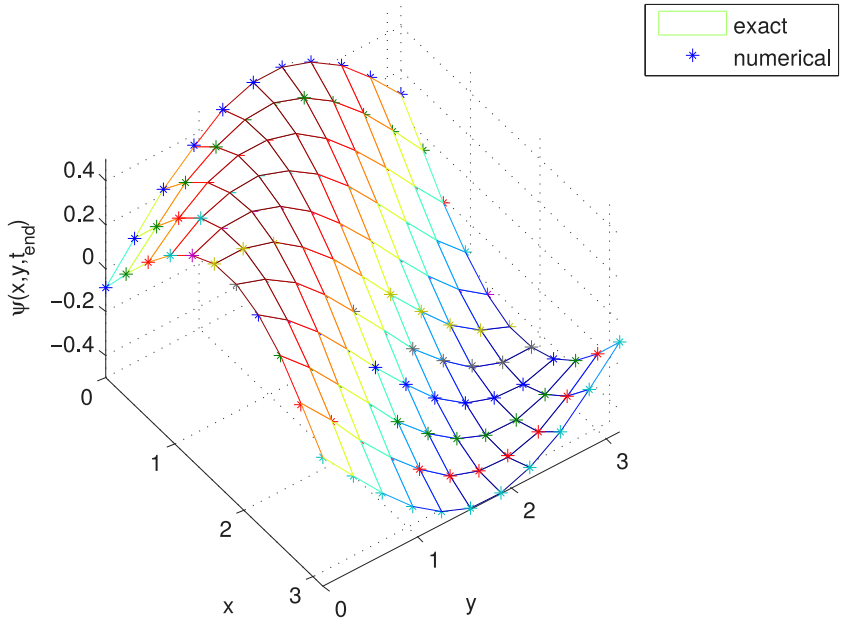

Fig. 2. Surface plot of the real part of the numerical and the exact solution at time $t = 1$ for Problem 3.2.

hand, we also check the conservation of mass of the proposed method on $x \in [-5, 20]$ and $t \in [0, 3]$. The errors are presented in different norms, namely L_1 and L_2. Table 1 shows that the proposed method is very efficient in terms of the conservation of mass.

In order to check the long time behaviour of the proposed method, we apply the proposed method on $x \in [-5, 20]$ and $t \in [0, 20]$. Table 2 emphasizes that the proposed method can be applied for a long time with accurate results.

Further, in order to compare the preservation of energy, we consider the exact and numerical solutions on $x \in [-5, 20]$ and $t \in [0, 20]$. For exact solution, we have

$$\int_{-20}^{5} |\psi|^2 dx = 4.0000, \quad \int_{-20}^{5} \left(-|\psi_x|^2 + \frac{|\psi|^4}{2}\right) dx = 1.1749,$$

while for the numerical solution, we have, at $t = 3$,

$$\int_{-20}^{5} |\psi|^2 dx = 4.0000, \quad \int_{-20}^{5} \left(-|\psi_x|^2 + \frac{|\psi|^4}{2}\right) dx = 1.1895.$$

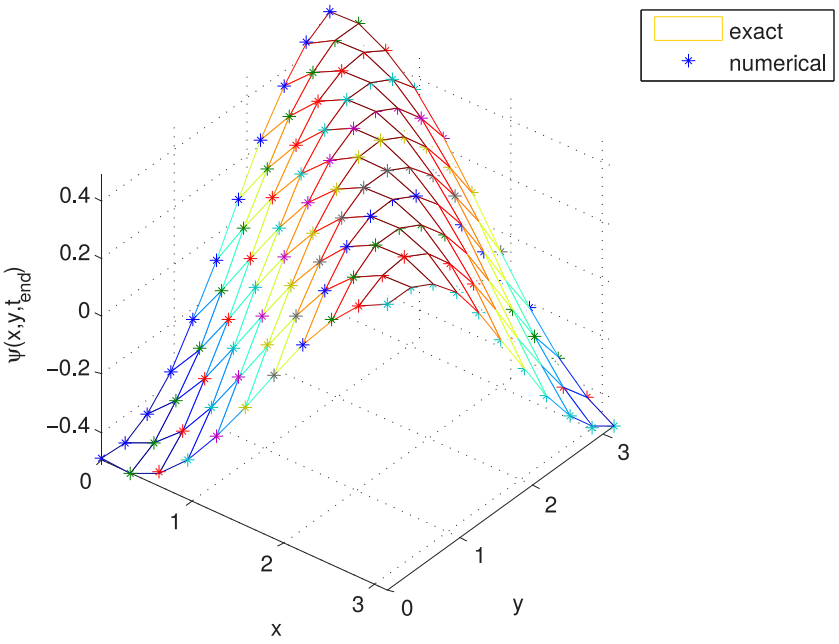

Fig. 3. Surface plot of the imaginary part of the numerical and the exact solution at time $t = 1$ for Problem 3.2.

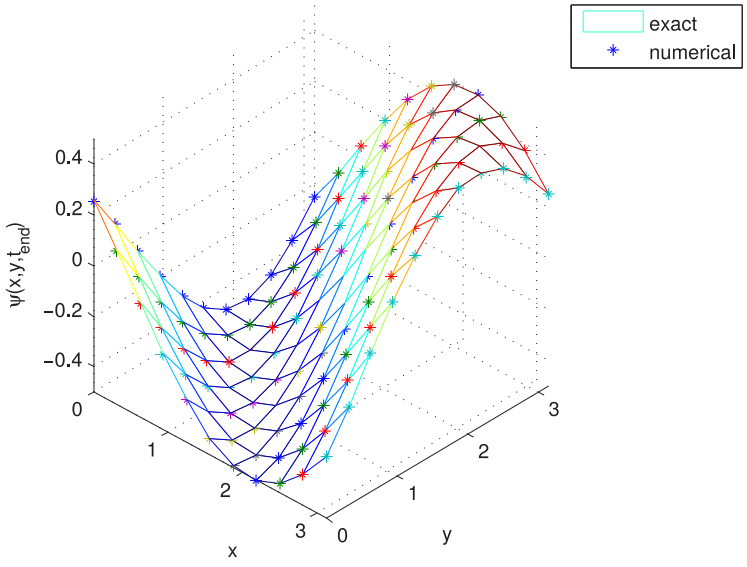

Fig. 4. Surface plot of the real part of the numerical and the exact solution at time $t = 3$ for Problem 3.2.

Table 1
Errors of mass conservation for different Δt and Δx where $x \in [-5, 20]$ and $t \in [0, 3]$ for Problem 3.1.

N	$\Delta t = 0.01$		$\Delta t = 0.001$	
	L_1	L_2	L_1	L_2
25	0.0023	2.8192e−04	0.0015	6.3240e−05
50	4.5138e−05	4.4278e−06	5.4477e−05	1.5920e−06
100	3.7685e−07	2.3124e−08	1.1644e−06	2.3856e−08
150	2.7268e−07	2.0663e−08	2.8687e−07	5.7848e−09

Moreover, at $t = 20$, we obtain

$$\int_{-20}^{5} |\psi|^2 dx = 3.9996, \quad \int_{-20}^{5} \left(-|\psi_x|^2 + \frac{|\psi|^4}{2}\right) dx = 1.1734,$$

which guarantees that the proposed method has the long-time behaviour not only for mass conservation but also for energy conservation.

3.2. Two-dimensional cubic nonlinear Schrödinger equation

Secondly, we consider the two-dimensional cubic nonlinear Schrödinger equation [20]:

$$i\frac{\partial \psi}{\partial t} + \frac{\partial^2 \psi}{\partial x^2} + \frac{\partial^2 \psi}{\partial y^2} + q|\psi|^2\psi = 0, \quad (x, y) \in [0, \pi]^2, \ t \in [0, 3] \tag{39}$$

with the exact solution of the given model [21,22]

$$\psi(x, y, t) = A \exp(i(k_1 x + k_2 y - \rho t)), \tag{40}$$

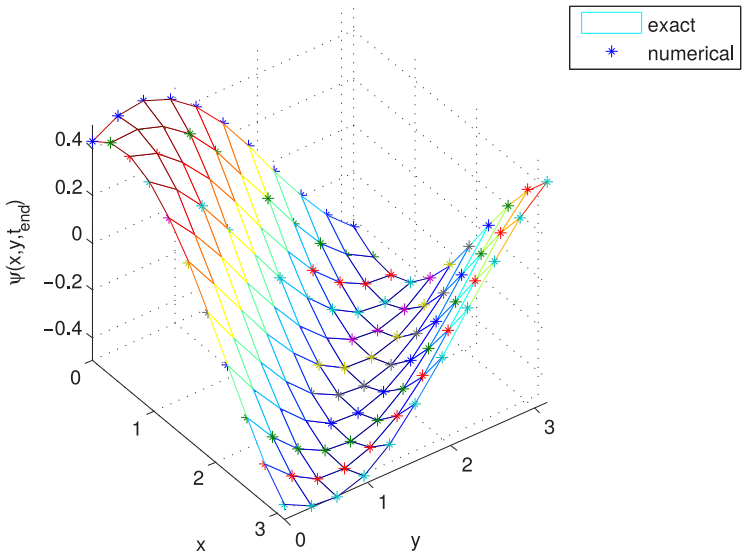

Fig. 5. Surface plot of the imaginary part of the numerical and the exact solution at time $t = 3$ for Problem 3.2.

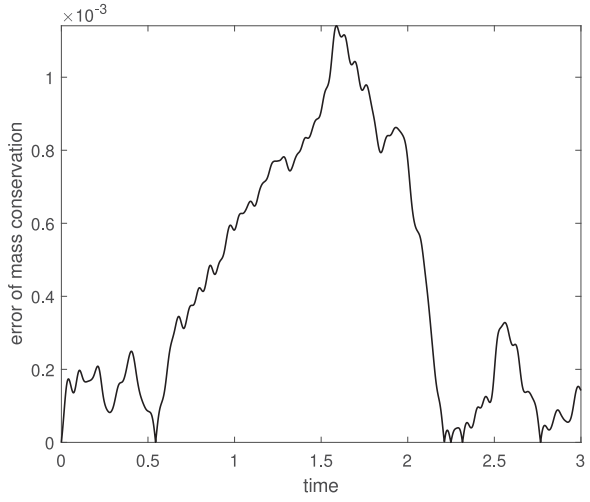

Fig. 6. Errors of mass conservations with $N = 16 \times 16$, $c_1 = c_2 = 0.7$, $\Omega = [0, \pi]^2$ and $t \in [0, 3]$ for Problem 3.2.

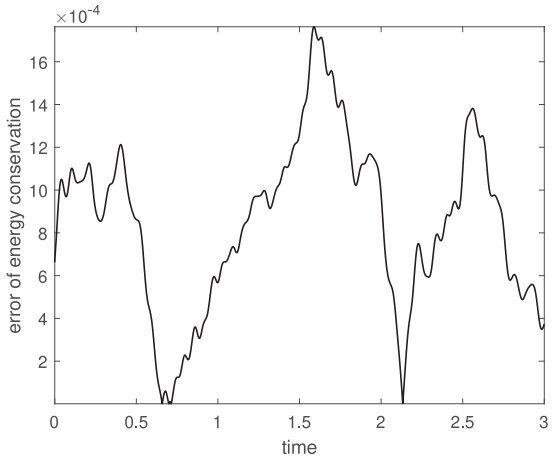

Fig. 7. Errors of energy conservations with $N = 16 \times 16$, $c_1 = c_2 = 0.7$, $\Omega = [0, \pi]^2$ and $t \in [0, 3]$ for Problem 3.2.

Table 2
Errors of mass conservation for different Δt and Δx where $x \in [-5, 20]$ and $t \in [0, 20]$ for Problem 3.1.

Δt	$N = 50$		$N = 100$	
	L_1	L_2	L_1	L_2
0.4	0.0444	0.0082	0.0169	0.0033
0.2	0.0218	0.0030	0.0030	6.7571e−04
0.1	0.0180	0.0180	0.0022	4.7494e−04
0.05	0.0180	0.0012	0.0020	3.1777e−04

where

$$\rho = {k_1}^2 + {k_2}^2 - q|A|^2, \tag{41}$$

subject to initial and boundary conditions

$$\psi(x, y, 0) = \psi_0(x, y), \quad (x, y) \in \Omega, \tag{42}$$

$$\psi(x, y, t) = g(x, y, t), \quad (x, y) \in \partial\Omega, \ t > 0, \tag{43}$$

where $\psi(x, y, t)$ is a complex function, $\Omega = [0, \pi]^2$ is a rectangular region and $\partial\Omega$ denotes the boundary of Ω.

The proposed method is applied to this example and the numerical results are shown in Table 3. The error norms L_1 and L_2 for the real and imaginary parts are presented with fixed number of collocation points $N = 10{\times}10$ at different times up to$t = 1$ with fixed $\Delta t = 0.001$. Numerical results are shown in Figs. 2 and 3 and it is evident from this figure that the solution obtained by the proposed method is in a perfect agreement with the exact solution. Here, meshfree method is used for discretizing the space derivatives and the linearization process which is defined by means of the Fréchet derivatives is used for time discretization where $N = 10 \times 10$ and the shape of the radial basis is 0.5. Moreover, initial and boundary conditions are chosen from the exact solution. In Table 4 error norms for different number of collocation points with t = 0.001 are shown. It can be observed that the accuracy of the method improves by increasing the number of collocation points.

In order to check the behaviour of the proposed method for long time, the numerical results at time $t = 3$ are shown in Figs. 4 and 5. From these figures, it is clear that the proposed method preserves the behaviour of the analytic solution for a long time. Table 5 gives the error at $t = 3$. This emphasizes that the proposed method is numerically stable. Figs. 6 and 7 show that the discrete energy and the discrete mass are well preserved.

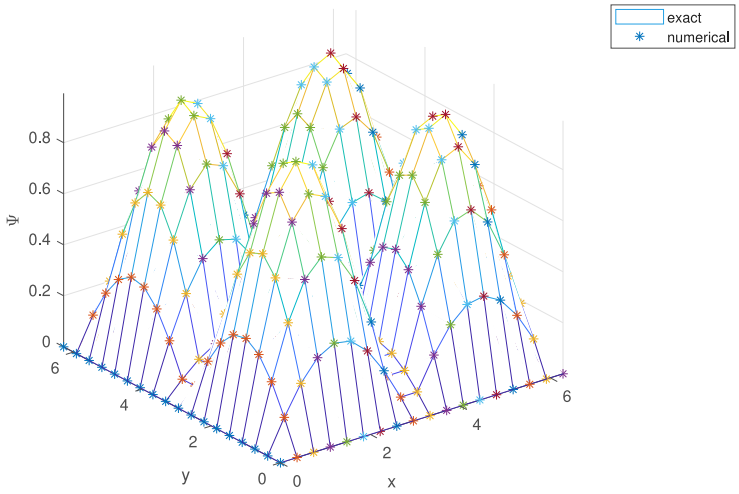

Fig. 8. Exact and numerical solutions of Eq. (44) at $t = 1$ with $N = 16 \times 16$ and $c_1 = c_2 = 0.7$ for Problem 3.3.

Table 3
Numerical errors for $N = 10 \times 10$ with $\Delta t = 0.001$ and $c_1 = c_2 = 0.5$ for Problem 3.2.

t	Real part		Imaginary part	
	L_1	L_2	L_1	L_2
0.1	1.2916e−02	6.1962e−03	4.1602e−03	2.1514e−03
0.2	1.8770e−02	9.6928e−03	4.7991e−03	2.4357e−03
0.3	2.2654e−02	1.2328e−02	4.2126e−03	2.3923e−03
0.4	1.9275e−02	1.1574e−02	4.8929e−03	3.3571e−03
0.5	2.0306e−02	1.4381e−02	7.4393e−03	4.8017e−03
0.6	2.4049e−02	1.5879e−02	7.4599e−03	5.6786e−03
0.7	2.8174e−02	1.8491e−02	8.6283e−03	5.4560e−03
0.8	3.0907e−02	2.3580e−02	6.7824e−03	4.6352e−03
0.9	3.4673e−02	2.7562e−02	4.8147e−03	3.4125e−03
1	3.8240e−02	2.8358e−02	4.2647e−03	2.9836e−03

Table 4
Error norms of the approximate solutions for $\Delta t = 0.001$ on $t \in [0, 1]$ with $c_1 = c_2 = 0.7$ for Problem 3.2.

t	$N = 8$		$N = 16$	
	L_1	L_2	L_1	L_2
0.1	8.2572e−03	5.0463e−03	1.6233e−03	8.4697e−04
0.2	1.4362e−02	8.0032e−03	1.4246e−03	8.9173e−04
0.3	1.9362e−02	1.0506e−02	2.1029e−03	1.3948e−03
0.4	1.9564e−02	1.3560e−02	2.4511e−03	1.4347e−03
0.5	2.3993e−02	1.7731e−02	1.9402e−03	1.2821e−03
0.6	3.0219e−02	2.2057e−02	1.8258e−03	1.1608e−03
0.7	3.5083e−02	2.4959e−02	1.8729e−03	1.0928e−03
0.8	3.7903e−02	2.6853e−02	1.6465e−03	1.0567e−03
0.9	4.1190e−02	2.8474e−02	1.9067e−03	1.1634e−03
1	4.0474e−02	2.9549e−02	2.4241e−03	1.5675e−03

3.3. Two-dimensional cubic nonlinear Schrödinger equation with an external potential

For the last example, we consider the two-dimensional cubic nonlinear Schrödinger equation

$$i\frac{\partial \psi}{\partial t} + \frac{1}{2}\left(\frac{\partial^2 \psi}{\partial x^2} + \frac{\partial^2 \psi}{\partial y^2}\right) - |\psi|^2\psi + \omega(x, y)\psi = 0, \quad (x, y) \in [0, 2\pi]^2,\ t \in [0, 1] \tag{44}$$

with an external potential

$$\omega(x, y) = -(1 - \sin^2 x \sin^2 y). \tag{45}$$

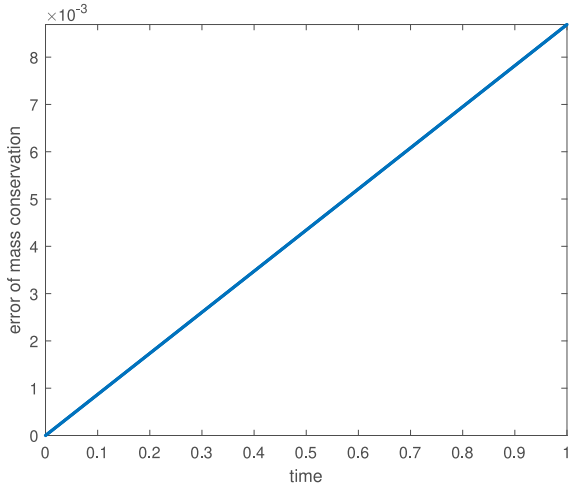

Fig. 9. Errors of mass conservation of Eq. (44) for Problem 3.3.

Table 5
Error norms of the approximate solutions at final time $t = 3$ with $c_1 = c_2 = 0.7$ for Problem 3.2.

N	Δt	L_1	L_2	CPU times
16 × 16	0.1	0.2305	0.1505	1.41
16 × 16	0.01	0.0175	0.0122	11.95
16 × 16	0.001	0.0027	0.0016	79.32

The exact solution is given in [21] as

$$\psi(x, y, t) = \sin x \sin y e^{-2it}. \tag{46}$$

The boundary and initial values are extracted from Eq. (46). The numerical experiments are performed for $(x, y) \in [0, 2\pi] \times [0, 2\pi]$ by collocating $N \times N = 16 \times 16$ for the shape parameter $c_1 = c_2 = 0.7$ and $t \in [0, 1]$ with various Δt values. The numerical errors in L_1 and L_2 norms and CPU times in seconds are given in Table 6.

The listed values in Table 6 show that the presented method remains stable for bigger choices of Δt values. Additionally, Fig. 8 indicates how well the approximate solutions fit the exact solution.

On the other hand, it is observed computationally and shown in Fig. 9 that in the case of presence of an external potential the proposed method may not preserve mass and, therefore, energy as well.

Table 6
Error norms of the approximate solutions at $t = 1$ with $x, y \in [0, 2\pi]^2$, $N = 16 \times 16$ and $c_1 = c_2 = 0.7$ for Problem 3.3.

N	Δt	L_1	L_2	CPU times
16×16	0.01	0.0477	0.0377	5.79
16×16	0.001	0.0047	0.0038	41.38
16×16	0.0001	4.7352e−04	3.7539e−04	278

4. Conclusion

In this paper, a new numerical method which is combination of Fréchet derivative and meshless method with radial basis functions is developed and applied to cubic nonlinear Schrödinger equation both in one- and two-dimensional cases. The numerical results confirm that the method is accurate and efficient. Moreover, the study has been enriched by considering the physical characteristic of the equation. The validation of the proposed method has also been tested on mass and energy conservation.

References

[1] Subaşı M. On the finite-differences schemes for the numerical solution of two dimensional Schrödinger equation. Numer Methods Partial Differential Equations 2002;18(6):752–8.
[2] Bratsos AG. A linearized finite-difference method for the solution of the nonlinear cubic Schrödinger equation. Korean J Comput Appl Math 2001;8:459–67.
[3] Wu L. Dufort–frankel-type methods for linear and nonlinear Schrödinger equations. SIAM J Numer Anal 1996;33:1526–33.
[4] Dehghan M, Taleei A. A compact split-step finite difference method for solving the nonlinear Schrödinger equations with constant and variable coefficients. Comput Phys Comm 2010;181(1):43–51.
[5] Dehghan M. Finite difference procedures for solving a problem arising in modeling and design of certain optoelectric devices. Math Comput Simul 2006;71(1):16–30.
[6] Taleei A, Dehghan M. Time splitting pseudo-spectral domain decomposition method for soliton solutions of the one- and multi-dimensional nonlinear Schrödinger equations. Comput Phys Comm 2014;185(6):1515–28.
[7] Iqbal A, Abd Hamid NN, Ismail AI Md. Numerical solution of nonlinear Schrödinger equation with Neumann boundary conditions using quintic B-spline Galerkin method. Symmetry 2019;11(4):469.
[8] Ersoy-Hepson Ö, Dağ İ. Numerical investigation of the solutions of Schrödinger equation with exponential cubic B-spline finite element method. Int J Nonlinear Sci Numer Simul 2021;22(2):119–33.
[9] Dehghan M, Abbaszadeh M. Solution of multi-dimensional Klein–Gordon-Zakharov and Schrödinger/Gross–Pitaevskii equations via local Radial Basis Functions-Differential Quadrature(RBF-DQ) techniqu on non-rectangular computational domains. Eng Anal Bound Elem 2018;92:156–70.
[10] Dehghan M, Mohammadi V. A numerical based on radial basis function finite difference(RBF-FD) technique for solving the high-dimensional nonlinear Schrödinger equations using an explicit time dicretization: Runge–Kutta method. Comput Phys Comm 2017;217:23–34.
[11] Kansa EJ. Multiquadrics - a scattered data approximation scheme with applications to computational fluid dynamics-II. Comput Math Appl 1990;19:147–61.
[12] Franke C, Schaback R. Convergence order estimates of meshless collocation methods using radial basis functions. Adv Comput Math 1998;8:381–99.
[13] Yao G, Siraj-ul-Islam, Sarler B. Assessment of global and local meshless methods based on collocation with radial basis functions for parabolic partial differential equations in three dimensions. Eng Anal Bound Elem 2012;36:1640–8.
[14] Dehghan M, Shokri A. A numerical method for solution of the two-dimensional sine-Gordon equation using the radial basis functions. Math Comput Simul 2008;79(3):700–15.
[15] Kansa EJ. Multiquadrics - a scattered data approximation scheme with applications to computational fluid dynamics-I. Comput Math Appl 1990;19:127–45.
[16] Ilati M, Dehghan M. DMLPG method for numerical simulation of soliton collisions in multi-dimensional coupled damped nonlinear Schrödinger system which ariese from Bose–Einstein condensates. Appl Math Comput 2019;346:244–53.
[17] Dehghan M, Mohammadi V. Two numerical meshless techniques based on radial basis functions (RBFs) and the method of generalied moving least squares (GMLS) for simulation of coupled Klein–Gordon-Schrödinger(KGS) equations. Comput Math Appl 2016;71(4):892–921.
[18] Fazel MR, Moghaddam MM, Poshtan J. Application of GDQ method in nonlinear manipulator undergoing large deformation. J Mech Eng Sci 2013;227(12):2671–85.
[19] Polyanin AD, Zaitsev VF. Handbook of nonlinear partial differential equations. Chapman and Hall/CRC; 2003.
[20] Abbasbandy S, Roohani Ghehsareh H, Hashim I. A meshfree method for the solution of two-dimensional cubic nonlinear Schrödinger equation. Eng Anal Bound Elem 2013;37:885–98.
[21] Xu Y, Zhang L. Alternating direction implicit method for solving two dimensional cubic nonlinear Schrödinger equation. Comput Phys Comm 2012;183:1082–93.
[22] Gao Z, Xie S. Fourth-order alternating direction implicit compact finite difference schemes for two-dimensional Schrödinger equations. Appl Numer Math 2011;61:593–614.